Available online at www.sciencedirect.com
ScienceDirect
Journal of Solid State Chemistry 179 (2006) 3949–3957
JOURNAL OF SOLID STATE CHEMISTRY
www.elsevier.com/locate/jssc

Electronic polarizability and crystallization of K_2O–TiO_2–GeO_2 glasses with high TiO_2 contents

T. Fukushima[a], Y. Benino[a], T. Fujiwara[b], V. Dimitrov[c], T. Komatsu[a,*]

[a]*Department of Materials Science and Technology, Nagaoka University of Technology, 1603-1Kamitomioka-cho, Nagaoka 940-2188, Japan*
[b]*Department of Applied Physics, Graduate School of Engineering, Tohoku University, 6-6-05 Aoba, Sendai 980-8579, Japan*
[c]*Department of Silicate Technology, University of Chemical Technology and Metallurgy, 8 Kl, Ohridki Blvd., Sofia 1756, Bulgaria*

Received 8 July 2006; received in revised form 26 August 2006; accepted 27 August 2006
Available online 9 September 2006

Abstract

Some K_2O–TiO_2–GeO_2 glasses with a large amount of TiO_2 contents (15–25 mol%) such as $25K_2O$–$25TiO_2$–$50GeO_2$ have been prepared, and their electronic polarizability, Raman scattering spectra, and crystallization behavior are examined to clarify thermal properties and structure of the glasses and to develop new nonlinear optical crystallized glasses. It is proposed that the glasses consist of the network of TiO_6 and GeO_4 polyhedra. The glasses show large optical basicities of $\Lambda = 0.88-0.92$, indicating the high polarizabity of TiO_n ($n = 4-6$) polyhedra in the glasses. $K_2TiGe_3O_9$ crystals are formed through crystallization in all glasses prepared in the present study. In particular, $20K_2O$–$20TiO_2$–$60GeO_2$ glass shows bulk crystallization and $18K_2O$–$18TiO_2$–$64GeO_2$ glass exhibits surface crystallization giving the *c*-axis orientation. The crystallized glasses show second harmonic generations (SHGs), and it is suggested that the distortion of TiO_6 octahedra in $K_2TiGe_3O_9$ crystals induces SHGs.

Keywords: Glass; Crystallization; Electronic polarizability; Raman scattering spectra; Second harmonic generation; $K_2TiGe_3O_9$

1. Introduction

In the area of photonics, transparent crystallized glasses consisting of nonlinear optical/ferroelectric crystals have received much attention, because such materials have a high potential for applications in laser hosts, tunable waveguides, tunable fiber gratings, and so on. In nonlinear optical crystals reported so far, there are many attractive TiO_2-based or-containing crystals, e.g., $BaTiO_3$ and $KTiOPO_4$. Adair et al. [1] demonstrated that TiO_2 shows the highest nonlinear refractive index in a large number of optical crystals, indicating a very high oxygen hyperpolarizability of Ti–O pairs. Dimitrov and Komatsu [2] indicated that TiO_2-based glasses have large oxide ion electronic polarizabilities. It is, therefore, of interest to fabricate glasses with a large amount of TiO_2 and to synthesis TiO_2-based nonlinear optical crystals through crystallization of such glasses. Indeed, there has been some reports on crystallized glasses consisting of nonlinear optical TiO_2-based crystals [3–16]. For instance, very recently, Kosaka et al. [7] demonstrated that crystallized glasses with $Ba_3Ti_3O_6(BO_3)_2$ crystals show a strong second harmonic intensity.

It is also noted that there has been some reports on the crystallized glasses consisting of GeO_2-based or-containing nonlinear optical crystals such as $LaBGeO_5$ and Bi_2GeO_5 [16–28]. In Table 1, some studies on the synthesis of TiO_2-based or GeO_2-based crystals in the crystallization processing of glasses reported so far are summarized [3–28]. Among them, it should be pointed out that transparent crystallized glasses with ferroelectric $Ba_2TiGe_2O_8$ crystals in the BaO–TiO_2–GeO_2 system show a large second-order optical nonlinearity of $d_{33} = \sim 20$ pm/V, being comparable to the values of $LiNbO_3$ single crystal, as reported by Takahashi et al. [15,16].

In this study, we focus our attention on K_2O–TiO_2–GeO_2 glasses containing both TiO_2 and GeO_2. It is known that the K_2O–TiO_2–GeO_2 system has a wide glass-forming region [29], meaning the possibility of the fabrication of

*Corresponding author. Fax: +81 258 47 9300.
E-mail address: komatsu@chem.nagaokaut.ac.jp (T. Komatsu).

0022-4596/$ - see front matter © 2006 Elsevier Inc. All rights reserved.
doi:10.1016/j.jssc.2006.08.035

glasses with a large amount of TiO_2. Since all oxides of K_2O, TiO_2, and GeO_2 have large oxide ion electronic polarizabilities [2,30,31], it is expected that K_2O–TiO_2–GeO_2 glasses would indicate high refractive indices and might have a possibility of the formation of optical nonlinear crystals through crystallization. Very recently, Grujic et al. [32] have reported some thermal properties and crystallization behavior of $20K_2O$–$20TiO_2$–$60GeO_2$ glass, but their information is limited. That is, there has been no report on physical properties such as refractive index, Raman scattering spectra, and nonlinear optical properties of crystallized samples for K_2O–TiO_2–GeO_2 glasses. The purpose of this study is to search new nonlinear optical crystallized glasses showing second harmonic generation (SHG) through investigation of the crystallization behavior of some K_2O–TiO_2–GeO_2 glasses with high TiO_2 contents. At the same time, the electronic polarizability of the ions and the established features in the Raman spectra and crystallized products are used to clarify the structure and nonlinear optical properties of the materials.

Table 1
TiO_2- or GeO_2-based glass systems and crystalline phases formed through crystallization reported so far

Glass system	Crystalline phase	Ref.
BaO–TiO_2–SiO_2(or TeO_2)	$BaTiO_3$	[3,4]
PbO–TiO_2–Al_2O_3–SiO_2	$PbTiO_3$	[5]
BaO–TiO_2–B_2O_3	$BaTi(BO_3)_2$, $Ba_3Ti_3O_6(BO_3)_2$	[6-8]
BaO–TiO_2–SiO_2	$Ba_2TiSi_2O_8$	[9,10]
Bi_2O_3–TiO_2–Nb_2O_5–B_2O_3–SiO_2	Bi_3TiNbO_9	[11]
Bi_2O_3–TiO_2–B_2O_3	$Bi_4Ti_3O_{12}$	[12]
K_2O–TiO_2–P_2O_5–SiO_2	$KTiOPO_4$	[13]
PbO–GeO_2	$Pb_5Ge_3O_{11}$	[17,18]
La_2O_3–B_2O_3–GeO_2	$LaBGeO_5$	[19-22]
Li_2O–B_2O_3–GeO_2	$LiBGeO_4$	[23]
Bi_2O_3–GeO_2–B_2O_3	Bi_2GeO_5	[24]
K_2O–Nb_2O_5–GeO_2	$K_{3.8}Nb_5Ge_3O_{20.4}$	[25,26]
BaO–Ga_2O_3–GeO_2	$Ba_3Ga_2Ge_4O_{14}$	[27,28]
BaO–TiO_2–GeO_2	$Ba_2TiGe_2O_8$	[14-16]
K_2O–TiO_2–GeO_2	$K_2TiGe_3O_9$	[32]
		Present study

2. Experimental

The chemical compositions of K_2O–TiO_2–GeO_2 glasses prepared in the present study are given in Table 2. Glasses were prepared by using a conventional melt-quenching method. Commercial powders of reagent grade K_2CO_3, TiO_2, and GeO_2 were mixed together and melted in a platinum crucible at 1250 °C for 1 h in an electric furnace. The melts were poured onto an iron plate and pressed to a thickness of 1–1.5 mm by another iron plate. Glass transition, T_g, crystallization onset, T_x, and crystallization peak, T_p, temperatures were determined using differential thermal analyses (DTA) at a heating rate of 10 K/min. Densities of glasses were determined with the Archimedes method using distilled water as an immersion liquid. Refractive indices at a wavelength of 632.8 nm (He–Ne laser) were measured at room temperature with a prism coupler (Metricon Model 2010).

The glasses were heat treated at various temperatures, and the crystalline phases present in the heat-treated samples were examined by X-ray diffraction (XRD) analysis at room temperature using Cu $K\alpha$ radiation and from Raman scattering spectra (Tokyo Instruments Co., Nanofinder operated at Ar^+ (488 nm) laser). Second harmonic generations (SHGs) of crystallized samples were examined by Maker fringe techniques [33]. A fundamental wavelength of a Q-switched Nd^{3+}: yttrium-aluminum-garnet (YAG) laser operating at $\lambda = 1064$ nm was used as the incident light, and the intensities of green light ($\lambda = 532$ nm) emissions were measured. As polarization for second harmonic (SH) intensity measurements, the combination of *p*-excitation and *p*-detection (*pp*-polarization) was used.

3. Results

3.1. Thermal properties of glasses

In this study, five different glasses such as $25K_2O$–$25TiO_2$–$50GeO_2$ (designated here as 50KTG glass), $20K_2O$–$20TiO_2$–$60GeO_2$ (60KTG), and $18K_2O$–$18TiO_2$–$64GeO_2$ (64KTG) were prepared, as shown in Table 2. Optically transparent bulk glasses were obtained for all compositions. DTA curves for some glasses are shown in

Table 2
Chemical compositions, glass transition, T_g, crystallization onset, T_x, and crystallization peak, T_p, temperatures, density d, and refractive index n of K_2O–TiO_2–GeO_2 glasses

Glass composition (mol%)				T_g (°C)	T_x (°C)	T_p (°C)	d (g/cm^3)	n
Sample	K_2O	TiO_2	GeO_2	±2	±2	±2	±0.002	±0.002
50KTG	25	25	50	515	596	612	3.344	1.705
60KTG	20	20	60	551	616	631	3.501	1.711
64KTG	18	18	64	554	636	651	3.574	1.716
60KTG-2	25	15	60	494	594	605	3.393	1.666
60KTG-3	15	25	60	559			3.591	1.766

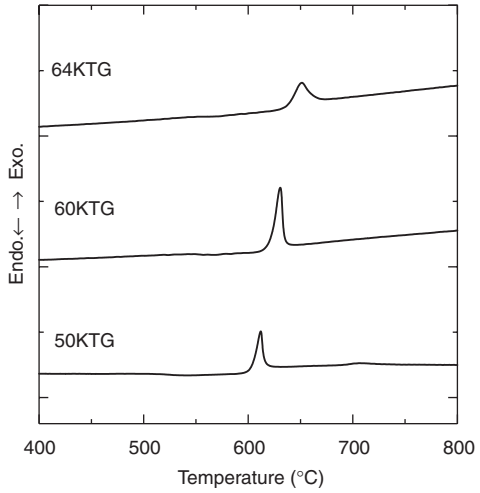

Fig. 1. DTA patterns for 50KTG, 60KTG, and 64 KTG glasses. Heating rate was 10 K/min. 50KTG: $25K_2O$–$25TiO_2$–$50GeO_2$, 60KTG: $20K_2O$–$20TiO_2$–$60GeO_2$, 64 KTG: $18K_2O$–$18TiO_2$–$64GeO_2$.

Fig. 1. It is seen that 60KTG glass shows a sharp crystallization peak. Contrary, in 64KTG glass, a broad crystallization peak is observed. These DTA data suggest that the crystallization behavior of K_2O–TiO_2–GeO_2 glasses is sensitive to the glass composition. The values of T_g, T_x, and T_p are summarized in Table 2, giving the values of $T_g = 494$–$559\,^{\circ}C$, $T_x = 594$–$636\,^{\circ}C$, and $T_p = 605$–$651\,^{\circ}C$. In xK_2O–$xTiO_2$–$(100-2x)GeO_2$ glasses, all values of T_g, T_x, and T_p increase with increasing GeO_2 content. In xK_2O–$(40-x)TiO_2$–$60GeO_2$ glasses, the values of T_g, T_x, and T_p increase with increasing TiO_2 content. Considering that generally K_2O, TiO_2 and GeO_2 in oxide glasses act as a network modifier, intermediate and network former, respectively, the composition dependence on these thermal properties (T_g and T_x) in K_2O–TiO_2–GeO_2 glasses would be reasonable.

The values of density, d, and refractive index, n, are given in Table 2. It is seen that both values in xK_2O–$xTiO_2$–$(100-2x)GeO_2$ glasses increase with increasing GeO_2 content. TiO_2 in xK_2O–$(40-x)TiO_2$–$60GeO_2$ glasses increases largely both density and refractive index. 60KTG glass, i.e., $20K_2O$–$20TiO_2$–$60GeO_2$ glass, for example, has the values of $d = 3.501\,g/cm^3$ and $n = 1.711$.

3.2. Eelectronic polarizability of glasses

One of the most important properties of materials, which is closely related to their applicability in the field of optics and electronics, is the electronic polarizability. Estimation of the state of polarizability of the ions is the subject of the so-called polarizability approach based on the Lorentz–Lorenz equation (Eq. (1)) giving the relationship between molar refraction, R_m, and refractive index, n:

$$R_m = \left[\frac{(n^2-1)}{(n^2+2)}\right]\left(\frac{M}{d}\right) = \left[\frac{(n^2-1)}{(n^2+2)}\right]V_m = \frac{4\pi\alpha_m N}{3}, \quad (1)$$

where M is the molecular weight, V_m is the molar volume, α_m the molar polarizability, and N the Avogadro's number. Eq. (1) gives the average molar refraction for isotropic substances such as liquids, glasses and cubic crystals. The Lorentz–Lorenz equation allows calculating the so-called the electronic polarizability of oxide ions, α_{O_2}-(n) in oxide materials by subtracting the cation polarizability from the molar polarizability α_m, taking into account the relationship proposed by Dimitrov and Sakka [30] for simple oxides and successfully applied for various oxide glasses [34,35]:

$$\alpha_{O_2}(n) = \left[\frac{R_m}{2.52} - \Sigma\alpha_i\right](N_{O^{2-}})^{-1} \quad (2)$$

where $\Sigma\alpha_i$ denotes molar cation polarizability and $N_{O^{2-}}$ denotes the number of oxide ions in the chemical formula. Furthermore, as discussed by Duffy [36], an intrinsic relationship exists between electronic polarizability of the oxide ions and so-called optical bacisity of the oxide medium, Λ, as given by Eq. (3):

$$\Lambda = 1.67\left(1 - \frac{1}{\alpha_{O^{2-}}}\right). \quad (3)$$

This relation presents a general trend toward an increase in the oxide ion polarizability with increasing optical basicity. The optical basicity of an oxide medium as proposed by Duffy and Ingram [37,38] is a numerical expression of the average electron donor power of the oxide species constituting the medium, and thus it is used as a measure of the acid–base properties of oxides, glasses, alloys, slags, molten salts, etc. Since increased oxide ion polarizability means stronger electron donor ability of oxide ions, the physical background of the oxide ion polarizability and optical basicity is naturally the same.

Using Eqs. (1), (2), and (3), we estimated the values of α_m, $\alpha_{O^{2-}}$ and Λ of K_2O–TiO_2–GeO_2 glasses prepared in the present study, and the results are shown in Table 3. The data of the cation polarizability of K^+, Ti^{4+} and Ge^{4+} are taken from Ref. [31]. As seen in Table 3, the glasses show the electronic polarizabilities of $\alpha_{O^{2-}} = 2.129 - 2.225\,Å^3$ and the optical basicities of $\Lambda = 0.886$–0.919, indicating by this manner that the glasses investigated in this study are basic in nature. In xK_2O–$xTiO_2$–$(100-2x)GeO_2$ glasses, the values of α_m, $\alpha_{O^{2-}}$ and Λ decrease with increasing GeO_2 content. On the other hand, in xK_2O–$(40-x)TiO_2$–$60GeO_2$ glasses, these values increase with increasing TiO_2 content. It is, therefore, considered that TiO_2 enhances the electronic polarizability in K_2O–TiO_2–GeO_2 glasses. The relatively large values of α_m, $\alpha_{O^{2-}}$ and Λ obtained in the present study suggest that K_2O–TiO_2–GeO_2 glasses have a high potential as nonlinear optical materials. The obtained values of the optical basicity of K_2O–TiO_2–GeO_2 glasses are close to those of other TiO_2-based glasses such as K_2O–TiO_2 and PbO–TiO_2 for which have been reported values of $\Lambda = 0.85$–1.17 [34]. Similarly, Kosaka et al. [7] reported that the BaO–TiO_2–B_2O_3 glasses with high TiO_2 contents of 30–40 mol% show large optical basicity of

Table 3
Molar volume V_m, mean atomic volume V_{atom}, calculated packing density V_p, molar polarizability α_m, electronic polarizability of oxide ions α_{O_2-}, and refractive index based optical basicity Λ of K_2O–TiO_2–GeO_2 glasses

Sample	V_m (cm^3/mol) ±0.03	V_{atom} (cm^3/g-atom) ±0.03	V_p ±0.03	α_m (Å^3) ±0.01	α_{O_2-} (Å^3) ±0.005	Λ ±0.003
50KTG	28.65	9.55	0.574	4.41	2.225	0.919
60KTG	27.87	9.29	0.568	4.32	2.155	0.895
64KTG	27.50	9.17	0.567	4.28	2.129	0.886
60KTG-2	28.97	9.66	0.561	4.27	2.145	0.891
60KTG-3	26.97	8.99	0.568	4.42	2.192	0.908

$\Lambda = 0.81$–0.87 due to the high polarizabity of TiO_n polyhedra ($n = 4$–6).

The values of molar volume, V_m, and mean atomic volume, V_{atom}, estimated from the values of density and chemical composition are shown in Table 3. It is seen that both values of V_m and V_{atom} in xK_2O–$xTiO_2$–$(100-2x)$-GeO_2 glasses decrease with increasing GeO_2 content. The ionic radii of K^+ (eight oxygen coordination number (CN)), Ti^{4+} (six CN) and Ge^{4+} (four CN) are 0.151, 0.0605, and 0.039 nm, respectively [39]. As the ionic radii of O^{2-}, the following values are taken from the consideration of coordination number; 0.142 nm in K_2O, 0.140 nm in TiO_2 and 0.138 nm in GeO_2 [39]. We calculated the volume occupied by constituent ions (K^+, Ti^{4+}, Ge^{4+}, O^{2-}) for a given composition by considering their ionic radius and coordination numbers, V_{cal}, and for instance, the values of $V_{cal} = 16.45\,cm^3$/mol for 50KTG, $V_{cal} = 15.84\,cm^3$/mol for 60KTG, and $V_{cal} = 15.59\,cm^3$/mol for 64KTG were obtained. In these calculations, the coordination number of Ge^{4+} is fixed to four for simplicity. Furthermore, we estimated the packing density, V_p, of a given composition from the following:

$$V_p = \frac{V_{cal}}{V_m}. \quad (4)$$

The values obtained are given in Table 3, indicating that all glasses have similar values of $V_p = 0.561$–0.574. It is, therefore, considered from the values of V_m, V_{atom}, and V_p that there is no drastic change in the glass structure in K_2O–TiO_2–GeO_2 glasses. In xK_2O–$xTiO_2$–$(100-2x)GeO_2$ glasses, however, the packing degree of constituent ions decreases very slightly with increasing GeO_2 content. Hoppe [40] has reported the values of 0.45–0.51 for the packing density of binary K_2O–GeO_2 glasses and discussed the coordination number of Ge^{4+} ions.

3.3. Raman scattering spectra of glasses

The Raman scattering spectra at room temperature for 50KTG, 60KTG, 64KTG, 60KTG-2, and 60KTG-3 glasses are shown in Figs. 2 and 3. Three main broad peaks are observed in all samples, i.e., at around 500, 750–765, and 865 cm^{-1}. Furthermore, two shoulder peaks are detected at around 580 and 920 cm^{-1}. As seen in Fig. 2, the relative intensities of the peaks at ~500 and 750–765 cm^{-1} increase with increasing GeO_2 content, and contrary, the relative intensity of the peak at 865 cm^{-1} decreases. For the glasses with a fixed GeO_2 content of 60 mol% but with different K_2O/TiO_2 ratios, the relative

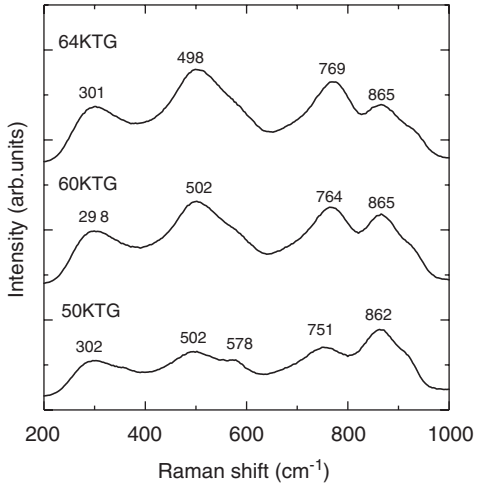

Fig. 2. Raman scattering spectra at room temperature for 50KTG, 60KTG, and 64 KTG glasses. 50KTG: $25K_2O$–$25TiO_2$–$50GeO_2$, 60KTG: $20K_2O$–$20TiO_2$–$60GeO_2$, 64 KTG: $18K_2O$–$18TiO_2$–$64GeO_2$.

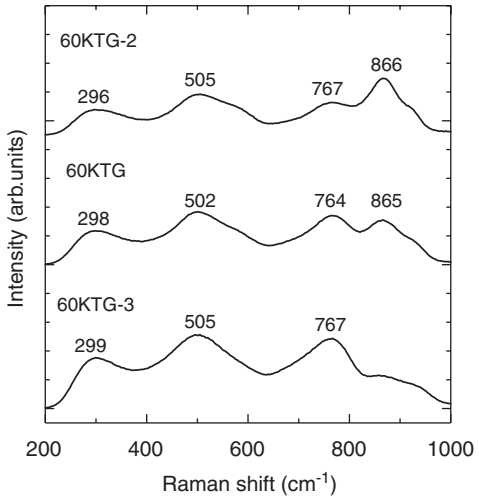

Fig. 3. Raman scattering spectra at room temperature for 60KTG, 60KTG-2, and 60KTG-3 glasses. 60KTG: $20K_2O$–$20TiO_2$–$60GeO_2$, 60KTG–2: $25K_2O$–$15TiO_2$–$60GeO_2$, 60 KTG–3: $15K_2O$–$25TiO_2$–$60GeO_2$.

intensity of the peak at ~765 cm^{-1} decreases largely with increasing K_2O/TiO_2 ratio, and contrary, the relative peak intensity at ~865 cm^{-1} increases.

So far, many Raman scattering spectra for GeO_2-based or TiO_2-containing glasses have been reported. For GeO_2-based glasses, Raman scattering spectra (i.e., peak position and intensity) relating to vibrations of GeO_4 tetrahedra change significantly depending on the type and amount of network modifier cations. Basically, however, for GeO_2-based glasses, bands in the mid-frequency region of ~400–500 cm^{-1} are assigned to symmetric stretching vibrations of Ge–O–Ge bonds (bridge) associated with four- and three-membered GeO_4 rings, and bands in the high-frequency region of 750–870 cm^{-1} are assigned to stretching vibrations of $Ge–O^-$ bonds (terminal groups) [41–46]. In particular, in alkali germanate glasses, increasing the amount of alkali content results in increasing concentration of non-bridging oxygen (NBO) atoms, and the bands at ~780 and ~870 cm^{-1} have been assigned to symmetric stretching motions of $Ge–O^-$ bonds involving two NBO atoms and one NBO atom, respectively. On the other hand, it is also well known that TiO_4 tetrahedra, TiO_5 square pyramid and TiO_6 octahedra in glasses show Raman active bands [47–53]. According to Furukawa and White [47], the frequencies for TiO_4 are around 750 cm^{-1}, while those for TiO_6 are less than 650 cm^{-1}. When TiO_4 units are polymerized, the frequencies of the Ti–O stretching modes would be expected to increase. On this basis they have assigned the bands at 910 and 880 cm^{-1} in the Raman spectra of $Li_2Si_2O_6$–TiO_2 glasses to Ti–O stretching vibrations of fourfold coordinated Ti^{4+} ions [47]. The previous studies [47–53] suggest the following peak assignments; 750–880 cm^{-1} for Ti–O stretching vibration of TiO_4, ~830–930 cm^{-1} for Ti–O stretching vibration of TiO_5, and ~630–740 cm^{-1} for Ti–O stretching vibration of TiO_6.

Considering the features of Raman scattering spectra for GeO_2-based and TiO_2-containing glasses [41–53], the spectra for K_2O–TiO_2–GeO_2 glasses shown in Figs. 2 and 3 are interpreted as follows. (1) The peaks at ~ 500 cm^{-1} are assigned to symmetric stretching vibrations of Ge–O–Ge bonds in interconnected GeO_4 tetrahedra. (2) The peaks at 750–765 cm^{-1} are assigned to stretching vibrations of $Ge–O^-$ bonds with two NBO atoms, and probable coordination polyhedra are $K\cdots O–Ge(O_2)–O\cdots Ti$. Furthemore, Ti–O stretching vibrations of TiO_n units with n less than 6 might contribute to these peaks of 750~765 cm^{-1}. (3) The peaks at ~ ~865 cm^{-1} are assigned to stretching vibrations of $Ge–O^-$ bonds with one NBO atom, and probable coordination polyhedra are $Ge(O_3)–O\cdots K$. (4) The peaks at ~865 cm^{-1} might include some contributions of Ti–O stretching vibrations of TiO_4 tetrahedra. (5) The two shoulder peaks at ~580 and 920 cm^{-1} might be related to the bending mode of Ge–O–Ge bridges involving motion of both O and Ge atoms [45] and to antisymmetric stretching of Ge–O–Ge bonds [46], respectively. The structure of K_2O–TiO_2–GeO_2 glasses, in particular the coordination state of Ti^{4+} ions will be discussed later.

3.4. Crystallization of glasses and second harmonic generation

The XRD patterns at room temperature for the bulk crystallized samples obtained by heat treatment at various temperatures in 60KTG glass ($T_g = 551\,^{\circ}C$, $T_x = 616\,^{\circ}C$) are shown in Fig. 4. It is seen that the crystallization occurs in the sample heat-treated at ~T_g for 3 h. All peaks are assigned to the $K_2TiGe_3O_9$ crystalline phase [54, JCPDS No.27-394]. It should be pointed out that the chemical composition of 60KTG glass, i.e., $20K_2O$–$20TiO_2$–$60GeO_2$, corresponds to the stoichiometric composition of the $K_2TiGe_3O_9$ phase. The XRD data shown in Fig. 4 indicate that the $K_2TiGe_3O_9$ phase is formed randomly at the surface of the glass without any orientation. From the XRD analyses for the pulverized samples, it was also confirmed that $K_2TiGe_3O_9$ crystals are formed in the interior of 60KTG glass, i.e., bulk crystallization. Grujic et al. [32] also reported the formation of $K_2TiGe_3O_9$ crystals in $20K_2O$–$20TiO_2$–$60GeO_2$ glass. The crystallized samples in 50KTG glass showed XRD patterns similar to the case of 60KTG glass, indicating the random orientation of $K_2TiGe_3O_9$ crystals at the surface and in the interior of 50KTG glass.

The XRD patterns for the bulk crystallized sample obtained by heat treatment at 559 °C for 3 h in 64KTG glass ($T_g = 554\,^{\circ}C$, $T_x = 636\,^{\circ}C$) are shown in Fig. 5, in which the surface of the bulk sample was polished. The peaks are assigned to the $K_2TiGe_3O_9$ crystalline phase. It is seen that $K_2TiGe_3O_9$ crystals are highly oriented at the surface, i.e., c-axis orientation. The scanning electron micrograph for the cross-section of this crystallized sample is shown in Fig. 6. The dense formation of crystals with a thickness of ~2 μm is confirmed, keeping a good optical

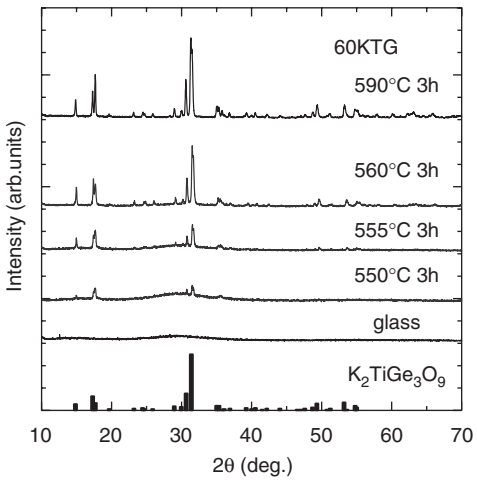

Fig. 4. Powder XRD patterns at room temperature for crystallized samples of 60KTG glass. The peaks are assigned to the $K_2TiGe_3O_9$ crystalline phasae. 60KTG: $20K_2O$–$20TiO_2$–$60GeO_2$.

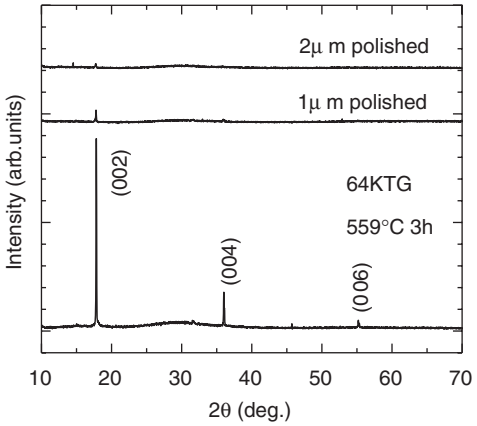

Fig. 5. Bulk XRD patterns at room temperature for crystallized samples of 64KTG glass. The crystalline phase is $K_2TiGe_3O_9$. 64KTG: $18K_2O$–$18TiO_2$–$64GeO_2$.

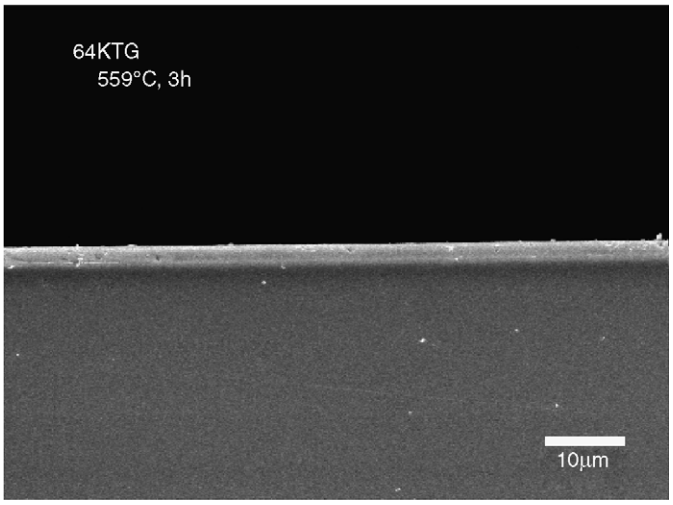

Fig. 6. SEM photograph for the cross-section of the crystallized sample of 64KTG glass. 64KTG: $18K_2O$–$18TiO_2$–$64GeO_2$.

transparency. In the sample heat-treated at a high temperature of 636 °C (crystallization temperature), $K_2TiGe_3O_9$ crystals are formed randomly in the interior of the glass.

We carried out SHG experiments for crystallized glasses consisting of $K_2TiGe_3O_9$ crystals. As an example, the Maker fringe pattern for the transparent surface crystallized sample obtained by heat treatment at 559 °C for 3 h in 64KTG glass is shown in Fig. 7. The SHG was clearly detected. Furthermore, it is seen that the SH intensity changes depending on the angle of incident light, indicating the orientation of polarized direction at the surface. SHGs were also confirmed in other crystallized samples of 60KTG and 50KTG glasses. No detectable SHGs were observed in the base K_2O–TiO_2–GeO_2 glasses (not crystallized samples) prepared in the present study. That is, the present study suggests that $K_2TiGe_3O_9$ crystals formed in K_2O–TiO_2–GeO_2 glasses might have some origin for inducing anisotropic polarizations in its structure. The structure of the $K_2TiGe_3O_9$ phase will be discussed later.

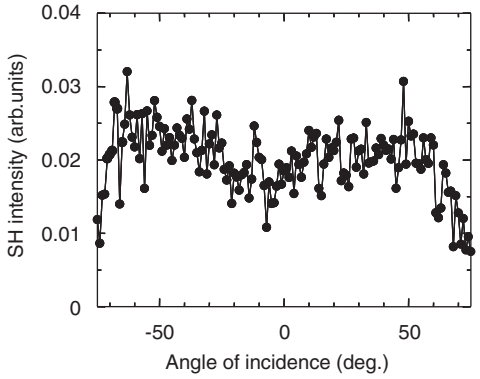

Fig. 7. Maker fringe pattern of SH intensity for the crystallized (559 °C, 3 h) sample of 64KTG glass. 64KTG: $18K_2O$–$18TiO_2$–$64GeO_2$.

3.5. Raman scattering spectra of crystallized glass and the $K_2TiGe_3O_9$ phase

The Raman scattering spectrum at room temperature for $K_2TiGe_3O_9$ polycrystalline samples prepared by a solid state reaction (550 °C, 10 h + 840 °C, 10 h, in air) in the present study are shown in Fig. 8. This is the first report on the Raman scattering spectrum for this crystal. It has been reported that the $K_2TiGe_3O_9$ phase has a trigonal structure with the lattice constants of $a = 1.191$ and $c = 1.001$ nm, space group of $P\bar{3}c1$ [54,55]. This phase consists of mixed tetrahedral-octahedral framework structures in which three-membered $[Ge_3O_9]$ rings of GeO_4 tetrahedra are interconnected by isolated TiO_6 octahedra via shared corners. That is, the $K_2TiGe_3O_9$ phase consists of mixed GeO_4 tetrahedral–TiO_6 octahedral framework structures [54,55].

As reported by Graves et al.[56], TiO_6 octahedron gives the following prominent Raman active bands: peaks at 470–490 cm^{-1} are assigned to torsional modes in Ti–O bonds, peak at ~650 cm^{-1} is associated with the symmetric stretching of Ti–O bonds. It is, therefore, considered that the peaks at 480 and 655 cm^{-1} shown in Fig. 8 are related to TiO_6 octahedra in the $K_2TiGe_3O_9$ phase. On the other hand, the peaks at 511 and 526 cm^{-1} are assigned to symmetric stretching vibrations of Ge–O–Ge bonds in interconnected GeO_4 tetrahedra in the $K_2TiGe_3O_9$ phase [41–46,50]. Furthermore, the peak at 808 cm^{-1} would be assigned to stretching vibrations of $Ge–O^-$ bonds with NBO atoms [41–46,50,57]. The peak at 404 cm^{-1} is probably assigned to bending vibrations of GeO_4 tetrahedra [57].

The Raman scattering spectra for 60KTG glass and crystallized (644 °C, 3 h) sample are shown in Fig. 8. These Raman scattering spectra also indicate that 60KTG glass gives the formation of $K_2TiGe_3O_9$ crystals through the crystallization. It is noted that both 60KTG glass and crystallized sample have the Raman bands at similar positions, implying structural similarities between the precursor glass and $K_2TiGe_3O_9$ crystal. That is, it is

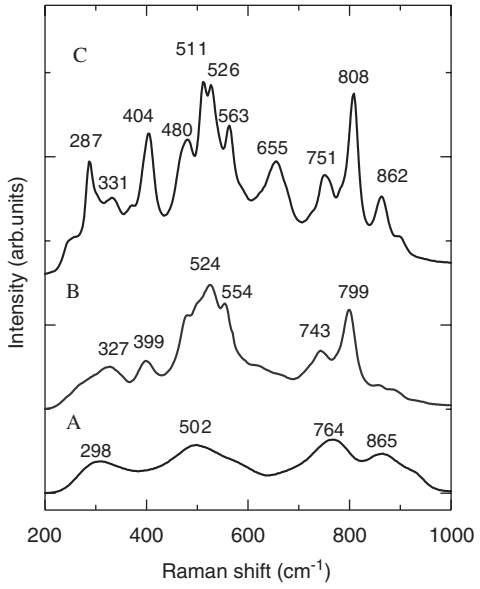

Fig. 8. Raman scattering spectra at room temperature for A: 60KTG glass, B: crystallized (644 °C, 3 h) sample of KTG glass, and C: $K_2TiGe_3O_9$ crystalline phase prepared by a solid state reaction. 60KTG: $20K_2O$–$20TiO_2$–$60GeO_2$.

suggested that K_2O–TiO_2–GeO_2 glasses examined in this study consist of the network of TiO_6 and GeO_4 polyhedra.

The Raman scattering spectrum for $K_2TiSi_3O_9$ crystals has been reported by Su et al. [52], and a strong peak at 964 cm^{-1} has been assigned to the vibration band of $Si(O_3)$–$O\cdots Ti(O_5)$ bond. As seen in Fig. 8, there is no peak at around 950 cm^{-1} in the Raman scattering spectrum for $K_2TiGe_3O_9$ crystals, but the peaks are observed below 900 cm^{-1}. These features indicate that the bond strength of $Ge(O_3)$–$O\cdots Ti(O_5)$, i.e., the connection between GeO_4 and TiO_6 polyhedra, in $K_2TiGe_3O_9$ crystals is smaller than that of $Si(O_3)$–$O\cdots Ti(O_5)$ in $K_2TiSi_3O_9$ crystals.

As seen in Table 2, 60KTG glass ($20K_2O$–$20TiO_2$–$60GeO_2$) has the values of $\Delta T = 65\,^{\circ}C$, where ΔT is the difference between crystallization and glass transition temperatures, i.e., $\Delta T = T_x - T_g$, and is known as an indicator for thermal stability against crystallization in glass. On the other hands, 50KTG and 64KTG glasses have the values of $\Delta T = 81$ and 82 °C, respectively. These results suggest that 60KTG glass with the composition corresponding to the stoichiometric $K_2TiGe_3O_9$ has a relatively low thermal stability against crystallization in K_2O–TiO_2–GeO_2 glasses. This might also support the structural similarity between 60KTG glass and $K_2TiGe_3O_9$ crystal.

4. Discussion

One of the main purposes of this study was to explore new transparent crystallized glasses showing SHGs in the ternary K_2O–TiO_2–GeO_2 glasses with high TiO_2 contents of 15–25 mol%. In the glasses examined in the present study, the crystalline phase formed through crystallization is $K_2TiGe_3O_9$. It should be pointed out that there is an inversion symmetry for the trigonal structure with a space group of $P\bar{3}c1$, meaning that in principle, the $K_2TiGe_3O_9$ phase would not show any second-order optical nonlinearities. But, SHGs were observed in the crystallized samples consisting of $K_2TiGe_3O_9$ crystals.

The structural unit of TiO_6 octahedron in the $K_2TiGe_3O_9$ phase is shown in Fig. 9. It is seen that the TiO_6 octahedron is not symmetrical, but is largely distorted. A ferroelectric origin in $BaTi_2O_5$ crystal has been proposed to be due to the distortion of TiO_6 octahedra [58,59]. It should be pointed out that at first the $BaTi_2O_5$ phase had been reported to have a centrosymmetric structure [60]. It is well known that a large second-order optical nonlinearity in transparent crystallized glasses consisting of fresnoite-type $Ba_2TiGe_2O_8$ crystals is induced by the presence of TiO_5 pyramidal units in the crystal structure [15,16,61]. Considering the relation between second-order optical nonlinearity/ferroelectricity and distortion of TiOn polyhedra in TiO_2-based crystals [15,16,58–61], it would be reasonable to conclude that SHGs in the crystallized samples of K_2O–TiO_2–GeO_2 glasses come from the distortion in TiO_6 octahedra in $K_2TiGe_3O_9$ crystals. Furthermore, it is considered that TiO_6 octahedra in K_2O–TiO_2–GeO_2 glasses might be distorted, consequently giving a strong effect on the electronic polarizability of the glasses.

The electronic polarizability of oxide ions and optical basicity in K_2O–TiO_2–GeO_2 glasses increase with increasing K_2O and TiO_2 or with decease of GeO_2 content. As reported by Dimitrov and Sakka [30], the simple oxides TiO_2 and GeO_2 have the following values: $\alpha_{O^{2-}} = 2.368\,Å^3$ and $\Lambda = 0.96$ for TiO_2 (rutile) and $\alpha_{O^{2-}} = 1.720\,Å^3$ and $\Lambda = 0.70$ for GeO_2. According to Duffy [62], optical basicity of K_2O is 1.4. That is the degree of basicity (electron donor ability of oxide ions) in simple oxides of K_2O, TiO_2, and GeO_2 is in the order: $GeO_2 < TiO_2 < K_2O$. The general trend that the electronic polarizability of oxide ions in K_2O–TiO_2–GeO_2 glasses increases with the

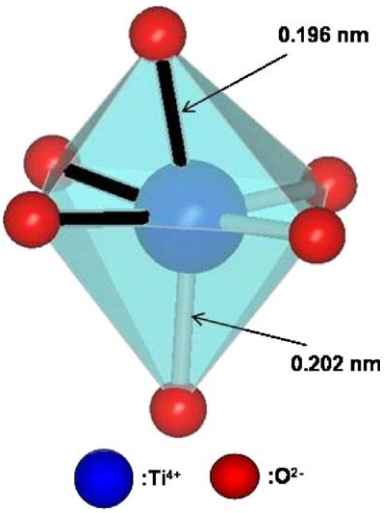

Fig. 9. TiO_6 octahedron in the $K_2TiGe_3O_9$ crystalline phase.

substitution of K_2O and TiO_2 for GeO_2 seems, therefore, to be reasonable. For example, $25K_2O$–$25TiO_2$–$50GeO_2$ glass possesses the highest values of $\alpha_{O^{2-}} = 2.25\,Å^3$ and $\Lambda = 0.919$. Dimitrov and Komatsu [63,64] applied the interaction parameter A proposed by Yamashita and Kurosawa [65] to describe the polarizability state of an average oxide ion in numerous simple oxides and binary oxide glasses and its ability to form an ionic–covalent bond with a cation. The interaction parameter is a quantitative measure for the interionic interaction of negative ions such as O^{2-} with the nearest neighbors (cations). They proposed the following values: $A = 0.081\,Å^{-3}$ for TiO_2 and $A = 0.146\,Å^{-3}$ for GeO_2 [63,64]. The increase in polarizability of the oxide ion as well as optical basicity of simple oxides or oxide glasses could be explained with decreased interaction inside the ionic pair, resulting in a smaller overlap between oxygen $2p$ and cation valence orbitals to form a chemical bond [63,64]. That is, the concept of interaction parameter suggest that Ti–O bonds are more ionic compared with Ge–O bonds. Considering the above, it is expected that the optical nonlinearity of K_2O–TiO_2–GeO_2 glasses with high TiO_2 contents is in close relation with the presence in the structure of TiO_n ($n = 4$–6) units with high polarizability.

Laudisio et al. [66] studied the devitrification behavior of Li_2O–TiO_2–GeO_2 glasses such as $20Li_2O$–$20TiO_2$–$60GeO_2$ (i.e., $Li_2TiGe_3O_9$), but the crystalline phases formed in the glasses with high TiO_2 contents have not been identified. To our knowledge, there has been no report on the synthesis (presence) of $Li_2TiGe_3O_9$ crystalline phase. As indicated in the present study, $K_2TiGe_3O_9$ crystals are formed easily through the crystallization of K_2O–TiO_2–GeO_2 glasses with high TiO_2 contents. In particular, as shown in Figs. 1 and 4, the glass with the composition corresponding to the stoichiometric $K_2TiGe_3O_9$ shows a prominent crystallization of $K_2TiGe_3O_9$.

Muller et al. [67] proposed that in the structure of various SiO_2-based glasses showing homogeneous nucleation both cationic and anionic arrangements in glass and crystal are similar. Although the microstructure of the crystallized glasses of $20K_2O$–$20TiO_2$–$60GeO_2$ has not been examined, the data shown in Figs. 1 and 4 suggest that the homogeneous nucleation occurs in this glass. It has been reported that the glass of $40BaO$–$20TiO_2$–$40SiO_2$ (i.e., $Ba_2TiSi_2O_8$) shows extremely high nucleation rates, giving nanocrystallized glasses consisting of nonlinear optical $Ba_2TiSi_2O_8$ nanocrystals [9,10,68]. Very recently, Gupta et al. [22] succeeded in developing transparent nanocrystallized glasses consisting of $LaBGeO_5$ nanocrystals through a two-step heat treatment in $25La_2O_3$–$25B_2O_3$–$50GeO_2$ (i.e., $LaBGeO_5$) glass. Furthermore, our research group [25,26] found that the glass of $25K_2O$–$25Nb_2O_5$–$50GeO_2$ shows a prominent nanocrystallization, in which the glass composition is close to that of $K_{3.8}Nb_5Ge_3O_{20.4}$ nanocrystals formed in that glass. Considering these previous studies, even in K_2O–TiO_2–GeO_2 glasses, we believe that some glasses, e.g., close to $20K_2O$–$20TiO_2$–$60GeO_2$, might show nanocrystallization through careful heat treatment and small modification of glass composition, and such a study is now under consideration.

5. Conclusions

K_2O–TiO_2–GeO_2 glasses with a large amount of TiO_2 contents (15–25 mol%) such as $25K_2O$–$25TiO_2$–$50GeO_2$ were prepared to search new nonlinear optical crystallized glasses showing second harmonic generations (SHGs). It was proposed from Raman scattering spectra that the glasses consist of the network of TiO_6 and GeO_4 polyhedra. The glasses showed large optical basicities of $\Lambda = 0.88$–0.92, indicating the high polarizabity of TiO_6 and GeO_4 polyhedra in the glasses. It was found from XRD analyses and Raman scattering spectra that $K_2TiGe_3O_9$ crystals were formed through crystallization. In particular, the surface crystallization giving the c-axis orientation of $K_2TiGe_3O_9$ crystals was found in $18K_2O$–$18TiO_2$–$64GeO_2$ glass. The crystallized glasses showed SHGs, and it was suggested that the distortion of TiO_6 octahedra in $K_2TiGe_3O_9$ crystals induces SHGs.

Acknowledgments

This work was supported from the SCOPE (Strategic Information and Communications R&D Promotion Program) project by the Ministry of Public Management, Home Affairs, Posts and Telecommunications, Japan, from the Grant-in-Aid for Scientific Research from the Ministry of Education, Science, Sport, Culture, and Technology, Japan, and from the 21st Century Center of Excellence (COE) Program in Nagaoka University of Technology.

References

[1] R. Adair, L.L. Chase, A.A. Payne, Phys. Rev. B 39 (1989) 3337.
[2] V. Dimitrov, T. Komatsu, J. Solid State Chem. 178 (2005) 831.
[3] A. Herczog, J. Am. Ceram. Soc. 47 (1964) 107.
[4] T. Komatsu, H. Tawarayama, K. Matusita, J. Ceram. Soc. Jpn. 101 (1993) 48.
[5] T. Kokubo, M. Tashiro, J. Non-Cryst. Solids 13 (1973/74) 328.
[6] A. Bhargava, J.E. Shelby, R.L. Snyder, J. Non-Cryst. Solids 102 (1988) 136.
[7] S. Kosaka, Y. Benino, T. Fujiwara, V. Dimitrov, T. Komatsu, J. Solid State Chem. 178 (2005) 2067.
[8] C.A.C. Feitosa, V.R. Mastelaro, A.R. Zanatta, A.C. Hernandes, E.D. Zanotto, Opt. Mater. 28 (2006) 935.
[9] A.A. Cabral, V.M. Fokin, E.D. Zanotto, C.R. Chinaglia, J. Non-Cryst. Solids 330 (2003) 174.
[10] Y. Takahashi, K. Kitamura, Y. Benino, T. Fujiwara, T. Komatsu, Appl. Phys. Lett. 86 (2005) 091110.
[11] K. Gerth, C. Rüssel, J. Non-Cryst. Solids 243 (1999) 52.
[12] K. Gerth, C. Rüssel, J. Non-Cryst. Solids 221 (1997) 10.
[13] V.N. Sigaev, P. Pernice, A. Aronne, O.V. Akimova, S.Yu. Stefanovich, A. Acaglione, J. Non-Cryst. Solids 292 (2001) 59.
[14] A. Halliyal, A.S. Bhalla, R.E. Newnham, L.E. Cross, J. Mater. Sci. 16 (1981) 1023.
[15] Y. Takahashi, Y. Benino, T. Fujiwara, T. Komatsu, Appl. Phys. Lett. 81 (2002) 223.

[16] Y. Takahashi, Y. Benino, T. Fujiwara, T. Komatsu, J. Appl. Phys. 95 (2004) 3503.
[17] A. Glass, K. Nassau, J.W. Shiever, J. Appl. Phys. 48 (1977) 5213.
[18] K. Pengpat, D. Holland, J. Eur. Ceram. Soc. 24 (2004) 2951.
[19] V.N. Sigaev, S.Yu. Stefanovich, P.D. Sarkisov, E.V. Lopatina, Glass Phys. Chem. 20 (1994) 398.
[20] Y. Takahashi, Y. Benino, T. Fujiwara, T. Komatsu, J. Appl. Phys. 89 (2001) 5282.
[21] Y. Takahashi, A. Iwasaki, Y. Benino, T. Fujiwara, T. Komatsu, Jpn. J. Appl. Phys. 41 (2002) 3771.
[22] P. Gupta, H. Jain, D.B. Williams, O. Kanert, R. Kuechler, J. Non-Cryst. Solids 349 (2004) 291.
[23] Y. Takahashi, Y. Benino, T. Fujiwara, K.B.R. Varma, T. Komatsu, J. Ceram. Soc. Jpn. 110 (2002) 22.
[24] K. Pengpat, D. Holland, J. Eur. Ceram. Soc. 23 (2003) 1599.
[25] F. Torres, K. Narita, Y. Benino, T. Fujiwara, T. Komatsu, J. Appl. Phys. 94 (2003) 5265.
[26] K. Narita, Y. Benino, T. Fujiwara, T. Komatsu, T. Hanada, Y. Hirotsu, J. Am. Ceram. Soc. 87 (2004) 113.
[27] Y. Takahashi, K. Saitoh, Y. Benino, T. Fujiwara, T. Komatsu, J. Ceram. Soc. Jpn. 112 (2004) 61.
[28] S. Kosaka, Y. Takahashi, Y. Benino, T. Fujiwara, T. Komatsu, Opt. Mater. 28 (2006) 1129.
[29] M. Imaoka, T. Yamazaki, J. Ceram. Soc. Jpn. 72 (1964) 182.
[30] V. Dimitrov, S. Sakka, J. Appl. Phys. 79 (1996) 1736.
[31] V. Dimitrov, T. Komatsu, J. Ceram. Soc. Jpn. 107 (1999) 879.
[32] S. Grujic, N. Blagojevic, M. Tosic, V. Zivanavic, B. Bozovic, J. Therm. Anal. Cal. 83 (2006) 463.
[33] S.K. Kurtz, T.T. Perry, J. Appl. Phys. 39 (1968) 3798.
[34] V. Dimitrov, T. Komatsu, J. Non-Cryst. Solids 249 (1999) 160.
[35] V. Dimitrov, T. Komatsu, J. Ceram. Soc. Jpn. 108 (2000) 330.
[36] J.A. Duffy, M.D. Ingram, J. Am. Chem. Soc. 93 (1971) 6448.
[37] J.A. Duffy, M.D. Ingram, J. Non-Cryst. Solids 21 (1976) 373.
[38] J.A. Duffy, J. Non-Cryst. Solids 109 (1989) 35.
[39] R.D. Shannon, Acta Crystallogr. A 32 (1976) 751.
[40] U. Hoppe, J. Non-Cryst. Solids 248 (1999) 11.
[41] H. Verweij, J.H.J.M. Buster, J. Non-Cryst. Solids 34 (1979) 81.
[42] G.S. Henderson, M.E. Fleet, J. Non-Cryst. Solids 134 (1991) 259.
[43] E.I. Kamitsos, Y.D. Yiannopoulos, M.A. Karakassides, G.D. Chryssikos, H. Jain, J. Phys. Chem. 100 (1996) 11755.
[44] D. Di Martino, L.F. Santos, A.C. Marques, R.M. Almeida, J. Non-Cryst. Solids 293–295 (2001) 394.
[45] G.S. Henderson, H. Wang, Eur. J. Min. 14 (2002) 733.
[46] G.S. Henderson, R.T. Amos, J. Non-Cryst. Solids 328 (2003) 1.
[47] T. Furukawa, W.B. White, Phys. Chem. Glasses 20 (1979) 69.
[48] A. Bhargava, R.L. Snyder, R.A. Condrate, Mater. Res. Bull. 22 (1987) 1603.
[49] S. Sakka, F. Miyaji, K. Fukumi, J. Non-Cryst. Solids 112 (1989) 64.
[50] A.A. Markgraf, S.K. Sharma, A.S. Bhalla, J. Am. Ceram. Soc. 75 (1992) 2630.
[51] S. Krimi, A. El Jazouli, L. Rabardel, M. Couzi, I. Mansouri, G. Le Flem, J. Solid State Chem. 102 (1993) 400.
[52] Y. Su, M.L. Balmer, B.C. Bunker, J. Phys. Chem. B 104 (2000) 8160.
[53] A. Tang, T. Hashimoto, T. Nishida, H. Nasu, K. Kamiya, J. Ceram. Soc. Jpn. 112 (2004) 496.
[54] J. Choisnet, A. Deschanvres, E.T.B. Raveau, J. Solid State Chem. 7 (1973) 408.
[55] M.E. Fleet, S. Muthupari, J. Solid State Chem. 140 (1998) 175.
[56] P.R. Graves, G. Hua, S. Myhra, J.G. Thompson, J. Solid State Chem. 114 (1995) 112.
[57] A. Rulmont, P. Tarte, J. Solid State Chem. 75 (1988) 244.
[58] Y. Akishige, K. Fukano, H. Shigematsu, Jpn. J. Appl. Phys. 42 (2003) L946.
[59] T. Kimura, T. Goto, H. Yamane, H. Iwata, T. Kajiwara, T. Akashi, Acta Crystallogr. C 59 (2003) 128.
[60] F.W. Harrison, Acta Crystallogr. 9 (1956) 495.
[61] N. Toyohara, Y. Benino, T. Fujiwara, S. Tanaka, K. Uematsu, T. Komatsu, Y. Takahashi, J. Appl. Phys. 99 (2006) 043515.
[62] J.A. Duffy, J. Am. Ceram. Soc. 80 (1997) 1416.
[63] V. Dimitrov, T. Komatsu, J. Ceram. Soc. Jpn. 107 (1999) 1012.
[64] V. Dimitrov, T. Komatsu, J. Ceram. Soc. Jpn. 108 (2000) 330.
[65] J. Yamashita, T. Kurosawa, J. Phys. Soc. Jpn. 10 (1955) 610.
[66] G. Laudiso, M. Catauro, A. Aronne, P. Pernice, Thermochim. Acta 294 (1997) 173.
[67] E. Muller, K. Heide, E.D. Zanotto, J. Non-Cryst. Solids 155 (1993) 56.
[68] Y. Takahashi, K. Kitamura, Y. Benino, T. Fujiwara, T. Komatsu, J. Ceram. Soc. Jpn. 113 (2005) 419.